Acta Cryst. (1993). B49, 67–72

Structure of the Incommensurate Composite Crystal $[Ba]_x[(Pt,Cu)O_3]$

BY KAZUTOSHI UKEI

Institute for Materials Research, Tohoku University, Katahira, Sendai 980, *Japan*

AKIJI YAMAMOTO

National Institute for Research in Inorganic Materials, Namiki 1, *Tsukuba* 305, *Japan*

AND YOUSUKE WATANABE, TOETSU SHISHIDO AND TSUGUO FUKUDA

Institute for Materials Research, Tohoku University, Katahira, Sendai 980, *Japan*

(*Received* 18 *January* 1991; *accepted* 30 *June* 1992)

Abstract

The nonstoichiometric compound $[Ba]_x[(Pt,Cu)O_3]$ ($x = 1.317$) has a composite crystal structure with $R^{P31c}_{111}:P^{R3m}_{1s}$, $a = 5.817$ (2), $c = 4.233$ (1) Å, $\mathbf{k} = (\mathbf{a}^* + \mathbf{b}^*)/3 + 1.519$ (1)$\mathbf{c}^*$, $V = 124.0$ Å^3, $Z_1 = 2$, $Z_2 = 3$, $D_x = 7.46$ Mg m^{-3}, Mo $K\alpha$, Cu $K\beta$, μ(Mo $K\alpha$) = 42.9 mm^{-1}. The structure was analyzed by a newly developed computer program based on the theory reported in a previous paper [Yamamoto (1992). *Acta Cryst.* A**48**, 476–483]. Final R factors: 0.075 (overall), 0.041 (main), 0.108 (first-order satellite), 0.102 (second-order satellite) and 0.224 (third-order satellite). The first subsystem, Ba, is located in the channels of the second columnar subsystem, $(Pt,Cu)O_3$, parallel to the c axis. Atomic position and Pt/Cu-atom occupancies are modulated along the c axis by the interaction between the two subsystems. Ba atoms are displaced helically while Pt/Cu atoms have a displacive modulation only along the c axis with rotational displacement of the coordinated O_3 atom clusters around the c axis. The first subsystem has a trigonal structure but with rhombohedral modulation because of the rhombohedral subsystem of $(Pt,Cu)O_3$. The possibility of a phase transition specific to the composite crystals is discussed.

Introduction

During synthesis of $ErBa_2Cu_3O_7$ single crystals by the flux method using a CuO flux in a platinum crucible, the title compound was obtained (Shishido, Ukei, Saito & Fukuda, 1992) and was found to be a new composite crystal.

In the previous paper (Yamamoto, 1992; hereinafter refered to as I) a simplified treatment of composite crystals in superspace is discussed. The method is applicable to all kinds of composite crystals. Although the setting of the unit vectors in the reciprocal space is much constrained compared with that based on the theory of Janner & Janssen (1980), the treatment in (I) is however still general and convenient for analyzing the composite crystal, as recognized by several authors (van Smaalen, 1989; Kato, 1990; Onoda, Kato, Gotoh & Oosawa, 1990). It is a similar method to that used in modulated structure analysis and the experience gained in the analysis of modulated structures can be applied to the analysis of composite crystal structures.

The structure of the new composite crystal obtained was analyzed using the method described in (I). It has a new superspace group $R^{P31c}_{111}:P^{R3m}_{1s}$. It consists of two modulated subsystems but their average structures have hexagonal and rhombohedral lattices. The structure has occupational and displacive modulations. Therefore this is one of the most general composite crystal structures. The modulation is very strong and satellite reflections up to the third order are observed. The success of the analysis of such a structure demonstrates the efficiency of the method. The composite structures may give a variety of phase transitions which have not been studied fully. One example of such a phase transition was found in $[AsF_6][Hg]_x[Hg]_x$ (Pouget, Shirane, Hastings, Heeger, Miro & MacDiarmid, 1978). The possibility of such a transition is discussed.

Experimental

The chemical composition of the specimen was determined, by energy-dispersive X-ray (EDX) analysis, to be $Ba_{4.0}Pt_{1.7}Cu_{1.1}O_x$. The sample chosen had dimensions 0.04 × 0.06 × 0.46 mm.

The integrated intensity data were collected on a Rigaku AFC-6A four-circle diffractometer using graphite-monochromatized Mo $K\alpha$ radiation, up to $2\theta = 55°$, with the ω–2θ scan mode [scan speed 4° min^{-1} (ω)]. During data collection, the intensities of three Bragg reflections were monitored after every

0108-7681/93/010067-06$06.00

© 1993 International Union of Crystallography

100 reflections measured, and no significant change in these intensities was observed throughout the experiment. Among 3625 measured reflections within the hemisphere, 631 unique reflections with $|F_o| \geq 3\sigma(|F_o|)$ were considered observed. $R_{int} = 0.068$. Corrections were applied for absorption ($5.25 < A^* < 14.18$) and for Lorentz and polarization effects, but not for extinction. The unit-cell dimensions were determined from the setting angles of 19 fundamental reflections ($23 < 2\theta < 26°$).

The crystal is composed of two kinds of twin domains which are related by a 180° rotation about the common c axis. As reflections from these twin domains appear close to each other, the integrated intensity for each reflection cannot be measured separately. The intensity profile data were measured using graphite-monochromatized Cu $K\beta$ radiation up to $2\theta = 62°$ with the step-scan mode along the c^* direction. The c^* component of the wavevector $\mathbf{k}$ was derived from six intensity profiles of these nearby reflections from two kinds of twin domains by least-squares profile fitting. The systematic absences of reflections were determined by the contributions from one kind of twin domain obtained by the intensity profile data.

Structure refinement

In the composite crystal, prominent reflections define two sets of three-dimensional reciprocal lattices of the two subsystems (Fig. 1). In the present case, the fundamental structure of the first subsystem has a hexagonal lattice with $a = 5.817$, $c = 4.233$ Å and the basis vectors of the reciprocal lattice are denoted by $\mathbf{a}^{*1}$, $\mathbf{b}^{*1}$ and $\mathbf{c}^{*1}$. The fundamental structure of the second subsystem has a rhombohedral lattice with unit vector given by $\mathbf{k}^1 = (\mathbf{a}^{*1} + \mathbf{b}^{*1})/3 + 1.519\mathbf{c}^{*1}$. If the hexagonal axes $\mathbf{a}^{*2} = (\mathbf{a}^{*1} + \mathbf{b}^{*1})/3$, $\mathbf{b}^{*2} = (-\mathbf{a}^{*1} + 2\mathbf{b}^{*1})/3$ and $\mathbf{c}^{*2} = 1.519\mathbf{c}^{*1}$ are adopted for the second subsystem, the unit vectors $\mathbf{a}^{*2}$ and $\mathbf{b}^{*2}$ are also used to index the main reflections of the first subsystem, instead of $\mathbf{a}^{*1}$ and $\mathbf{b}^{*1}$. This is the standard setting of the unit vectors in the case of the modulated structure with the wavevector $\mathbf{k}^1 = (\mathbf{a}^{*1} + \mathbf{b}^{*1})/3 + \gamma\mathbf{c}^{*1}$ (de Wolff, Janssen & Janner, 1981). Since the choice of the reciprocal basis vectors common to the two subsystems is recommended in (I), $\mathbf{a}^{*2}$, $\mathbf{b}^{*2}$, $\mathbf{c}^{*1}$ and $\mathbf{c}^{*2}$ were selected as the unit vectors for indexing reflections and recognized as the projection of the unit vectors in the four-dimensional reciprocal lattice onto three-dimensional external space $[\mathbf{d}^*_1, \mathbf{d}^*_2, \mathbf{d}^*_3, \mathbf{d}^*_4]^e$, where the superscript e means the external component of a four-dimensional vector. The unit vectors reciprocal to $\mathbf{d}^*_i$ ($i = 1, 2, 3, 4$) are written as $\mathbf{d}_i$ and their projection onto the external space is written as $\mathbf{d}_i^e$. The observed reflection with the diffraction vector $\mathbf{h}^e$ is indexed as $\mathbf{h}^e = \sum_{i=1}^4 h_i \mathbf{d}^{*e}_i$ and it is regarded as the projection of the four-dimensional lattice vector $\sum_{i=1}^4 h_i \mathbf{d}^*_i$ onto the external space. In the following sections we use $hklm$ for the indices of reflections, instead of $h_1h_2h_3h_4$. The jth ($j = 1, 2$) subsystem is described with reference to $P^j\mathbf{d}_i = \mathbf{d}_i^j$, where P^1 is the identity permutation (1) and P^2 is the permutation (3,4). Then the symmetry operator for the second subsystem is obtained from that for the first one by the permutation described in (I).

The superspace groups deduced from the reflection conditions ($l = 2n$ for $h0lm$ and $0klm$, and $h - k - m = 3n$ for $hklm$) and the Laue symmetry ($\bar{3}m$) are R^{P31c}_{111} or $R^{P\bar{3}1c}_{111}$ for the first subsystem and P^{R3m}_{1s} or $P^{R\bar{3}m}_{1s}$ for the second one (de Wolff *et al.*, 1981; Table 1 in I). Therefore the possible superspace group is either R^{P31c}_{111}:P^{R3m}_{1s} or $R^{P\bar{3}1c}_{111}$:$P^{R\bar{3}m}_{1s}$. The former was adopted in the later stages of the structure determination.

Approximate coordinates of Pt/Cu and Ba ions in the average structure were determined by direct methods with *RANTAN* (Yao, 1981), those of the other atoms were derived from trial models. *REMOS*90 (Yamamoto, 1992), a new version of a computer program for the refinement of average and modulated structures by the least-squares method (Yamamoto, 1982*a*), was used for the refinement. The average structure analysis showed that Ba atoms take a trigonal structure with $P31c$ and are located at

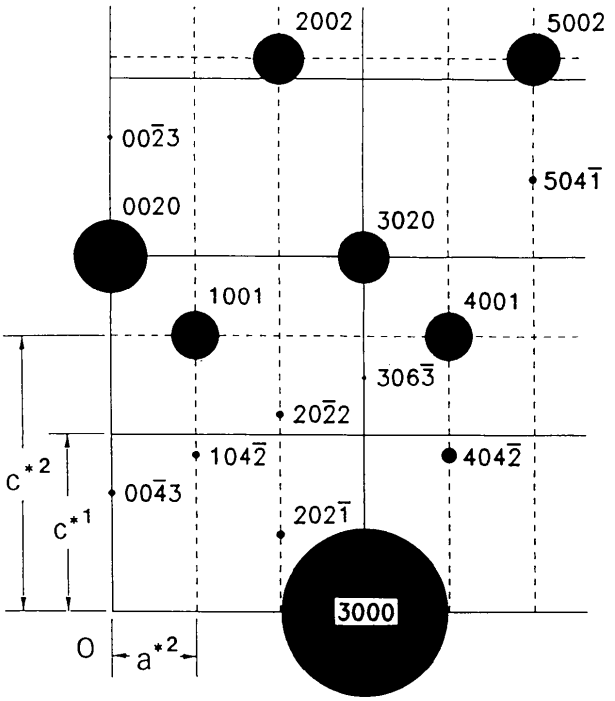

Fig. 1. A schematic view of the diffraction pattern from $[Ba]_x[(Pt,Cu)O_3]$. The radii of the discs are proportional to $|F_o|$.

Table 1. *Fourier coefficients forbidden or constrained by the site symmetry*

In the third column u, v and w, B and p represent the displacements along the a, b and c axes, the isotropic temperature factor and the occupation probability, respectively. d represents the displacement on the mirror plane perpendicular to the b axis.

Atom	Site symmetry	Modulation	
Ba	$\begin{pmatrix} 3 \\ t \end{pmatrix}$	u, v	Helical displacement with n mod(3) $\neq 0$ allowed
		w, B	n mod(3) $\neq 0$ forbidden
Pt/Cu	$\begin{pmatrix} 3m \\ 1s \end{pmatrix}$	u, v	Forbidden
		w, B, p	n mod(2) $\neq 0$ forbidden
O	$\begin{pmatrix} m \\ s \end{pmatrix}$	v	n mod(2) = 0 forbidden
		d, B	n mod(2) $\neq 0$ forbidden

the Wyckoff position 2(b), while (Pt,Cu)O_3 takes a rhombohedral structure with $R3m$, in which the Pt and Cu atoms occupy the same position at 3(a) and the O-atom occupation position at 9(b).

In general there exists a deviation from the average structure, because of the interaction between two subsystems, which causes satellite reflections. The order of the satellite reflections is expressed by min($|l|$,$|m|$) in this paper. $hkl0$ and $hk0m$ are the main reflections while $hkl1$ ($|l| > 0$) and $hk1m$ ($|m| > 0$) are the first-order satellites, $hkl2$ ($|l| > 1$) and $hk2m$ ($|m| > 1$) are the second-order satellites and so on. Satellite reflections up to the third order were observed in the present case, although the incommensurate composite crystals analyzed so far show no satellite reflections (Kato, 1990; Onoda *et al.*, 1990) and satellite reflections have been observed only in commensurate composite crystals that have two sets of lattices commensurate to each other (Onoda & Kato, 1991).

In the jth modulated subsystem, the x, y and z components of the displacement (u, v, w) with reference to $\mathbf{d}^j$, the isotropic temperature factor B and the occupation probability p of an atom are described in terms of a Fourier series as follows:

$$C^j(\bar{x}^j_4) = A_0 + \sum_{n=1}^{m}[A_n\cos(2\pi n\bar{x}^j_4) + B_n\sin(2\pi n\bar{x}^j_4)], \quad (1)$$

where $C^j = u^j$, v^j, w^j, B^j or p^j, $\bar{x}^j_4 = \mathbf{d}^*_4{}^j\cdot(\mathbf{X}^j + \bar{\mathbf{x}}^j)$ with $\mathbf{X}^j$ the lattice vector and $\bar{\mathbf{x}}^j$ the position vector in the fundamental structure, a bar denotes quantities belonging to the fundamental structure, and m is the maximum order of harmonics. The Fourier amplitude of the nth-order harmonic in a subsystem mainly contributes to the nth-order satellite reflections of that subsystem. However the nth-order satellite reflections of the first subsystem $hk0n$ overlap the main reflections of the second one and those of the second $hkn0$ overlap the main reflections of the first. Thus even when no satellite reflection is observed, the modulation waves can in principle be determined from the main reflections (Kato, 1990). Therefore the Fourier amplitudes up to the fourth order were taken into account in the present analysis.

Since all the atoms are in special positions, some Fourier coefficients are forbidden or constrained by the site symmetry (Yamamoto & Nakazawa, 1981; Yamamoto, 1982*b*), as shown in Table 1. In particular, a Pt/Cu atom is displaced only along the $\bar{c}$ axis, while only a helical displacement is allowed for Ba ions in the ab plane. In the latter, Fourier coefficients A_n, B_n for the helical displacement are expressed in terms of two parameters, C_n and D_n, as follows.

$$\begin{aligned} u(\bar{x}_4) = {} & (3^{1/2}C_1 + D_1)\cos(2\pi\bar{x}_4) \\ & + (-C_1 + 3^{1/2}D_1)\sin(2\pi\bar{x}_4) \\ & + (3^{1/2}C_2 - D_2)\cos(4\pi\bar{x}_4) \\ & + (C_2 + 3^{1/2}D_2)\sin(4\pi\bar{x}_4) \\ & + (3^{1/2}C_4 + D_4)\cos(8\pi\bar{x}_4) \\ & + (-C_4 + 3^{1/2}D_4)\sin(8\pi\bar{x}_4) \end{aligned}$$

$$\begin{aligned} v(\bar{x}_4) = {} & 2D_1\cos(2\pi\bar{x}_4) - 2C_1\sin(2\pi\bar{x}_4) \\ & - 2D_2\cos(4\pi\bar{x}_4) + 2C_2\sin(4\pi\bar{x}_4) \\ & + 2D_4\cos(8\pi\bar{x}_4) - 2C_4\sin(8\pi\bar{x}_4). \end{aligned} \quad (2)$$

Substitutional modulation is assumed for the occupation probability of a Pt/Cu atom; the occupation probability of a Cu atom is given by $1 - p$ when that of Pt is p.

The refinement has been made using the integrated intensity including the contributions from both kinds of twin domains, which are not measured separately. Since the $\mathbf{c}^{*1}$ component of $\mathbf{k}^1$ is nearly equal to 3/2 and the reflection condition for $hklm$ is $h - k - m = 3n$, reflections coming from the 180° twin domain with $\bar{h}\bar{k}lm$, $\bar{h}\bar{k}l \pm 3m \mp 2$ and $\bar{h}\bar{k}l \pm 6m \mp 4$ appear near the reflection $hklm$ when $h - k = 3n$, $3n \pm 1$ and $3n \mp 1$ respectively; these are integrated in the reflection $hklm$. The total intensity of these reflections is calculated in the program and compared with the intensity of the observed reflection $hklm$. The refinement by the full-matrix least-squares method on $|F|$ converged with R factors of 0.075 (overall), 0.041 (main), 0.108 (first-order satellite), 0.102 (second-order satellite) and 0.224 (third-order satellite) with the volume ratio of the twin domains being 0.64:0.36. Final parameters are listed in Table 2.†

In addition to *RANTAN* and *REMOS*90, the *UNICS*III program system (Sakurai & Kobayashi, 1979) and the full-matrix least-squares program

† A list of observed and calculated structure factors has been deposited with the British Library Document Supply Centre as Supplementary Publication No. SUP 55386 (6 pp.). Copies may be obtained through The Technical Editor, International Union of Crystallography, 5 Abbey Square, Chester CH1 2HU, England.

Table 2. *Final Fourier coefficients of the modulation waves*

The values have been multiplied by 10^2 for the displacement from the fundamental structure, by 10 for occupational parameters. The positions in the fundamental structure are (1/3, 0, 0), (0, 0, 0) and (0.14, 0.07, 1/2) for Ba, Pt/Cu and O atoms, respectively. Parameters constrained by the site symmetry are indicated by asterisks. The Fourier coefficients A_0 for the displacements of Ba and Pt/Cu atoms along the c axis are set to zero in order to fix the origin. The standard deviations are in parentheses.

		A_0	A_1	B_1	A_2	B_2	A_3	B_3	A_4	B_4
Ba	u		1.64 (5)*	−0.53 (8)*	0.67 (6)*	0.83 (8)*			−0.2 (1)*	−0.27 (9)*
	v		0.36 (9)*	−1.69 (3)*	−0.39 (9)*	1.00 (4)*			−0.35 (8)*	0.1 (1)*
	w	0					0.3 (2)	−0.3 (1)		
	B	1.12 (4)					0.11 (9)	−0.7 (1)		
Pt/Cu	u									
	v									
	w	0			−0.2 (5)	4.7 (2)			−0.4 (4)	5.7 (2)
	B	2.2 (1)			2.8 (2)	−0.6 (3)			1.5 (2)	−1.1 (2)
	p	5.7 (1)			−2.9 (3)	1.6 (5)			−0.1 (2)	−0.2 (4)
O	u	1.1 (3)*			0.3 (5)*	1.2 (4)*			0.6 (5)*	0.2 (4)*
	v	0.5 (2)*	9.3 (5)	1.7 (7)	0.2 (2)*	0.6 (2)*	−2.2 (5)	−2.3 (5)	0.3 (2)*	0.1 (2)*
	w	1 (1)			6 (2)	−6 (1)			−1 (2)	2 (1)
	B	4 (1)			−4 (1)	−5 (2)			−1 (1)	2 (1)

RADIEL (Coppens, Guru Row, Leung, Stevens, Becker & Yang, 1979) were also used during the analysis. Atomic scattering factors for the O^{2-} ion were taken from Tokonami (1965) and those for other ions were taken from *International Tables for X-ray Crystallography* (1974, Vol. IV, pp. 79, 86, 93, 149–150).

Discussion

The projection of the fundamental structure along the c axis is shown in Fig. 2. The perspective view of the modulated structure is shown in Fig. 3. As seen in the figure, O atoms in the $[(Pt,Cu)_3]_\infty$ column are rotated around the c axis forming the structure depicted in Fig. 4. Ba ions in the channels of the columns are displaced helically as mentioned before. The modulation of two adjacent Ba atoms along the c axis is almost antiphase because the $\mathbf{c}^{*1}$ component of $\mathbf{k}^1$ is 1.519, which is equivalent to 0.519. Since its difference from 1/2 is very small, the displacement normal to the c axis varies very slowly along the c axis. Similarly, the O_3 triangle rotates around the c axis at a period of almost $3c^2$ along the c axis, because the wavevector for the second subsystem is $\mathbf{c}^{*2}/1.519 \simeq 2\mathbf{c}^{*2}/3$. Some interatomic distances and angles for the atoms shown in Fig. 4 are presented in Table 3.

Fig. 5 shows the variations of the occupation probability of Pt atoms, the displacement parallel to the c axis of Pt/Cu atoms and the rotation angle of O atoms around the c axis from the mirror plane along the c direction. As shown in Fig. 6, there exists a correlation between the occupation probability of Pt/Cu atoms and the twist angle of the coordination polyhedra of O atoms. If the twist angle is large, a Pt/Cu atom has an octahedral coordination because the two adjacent O_3 triangles along the c axis rotate in opposite directions and, if the twist angle is small, it has a trigonal prismatic coordination. The Pt ion tends to possess octahedral coordination.

The mean occupation probability of Pt atoms obtained by the refinement and the ratio of the c axes of the two subsystems leads to the chemical composition $[Ba]_{1.3}[(Pt_{0.57}Cu_{0.43})O_3] \simeq Ba_{3.9}Pt_{1.7}Cu_{1.3}O_9$, which agrees well with the result of EDX analysis.

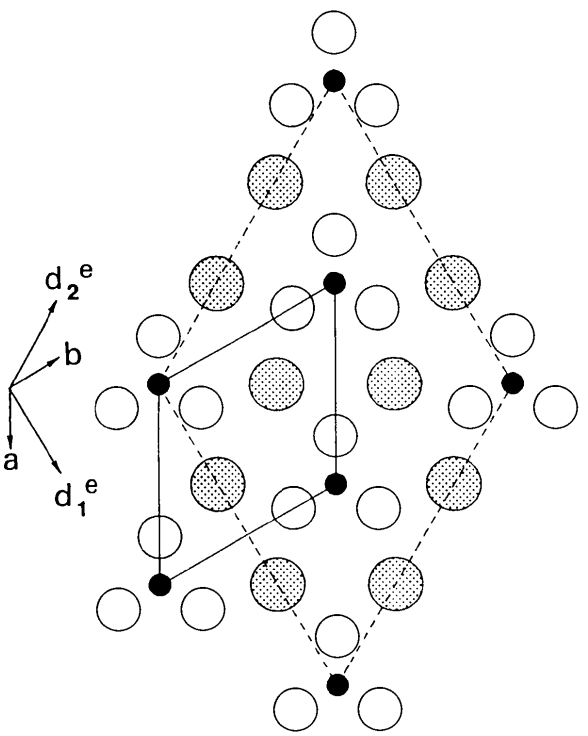

Fig. 2. A view of the fundamental structure along the c axis. Dotted, filled and open circles represent Ba, Pt/Cu and O atoms respectively.

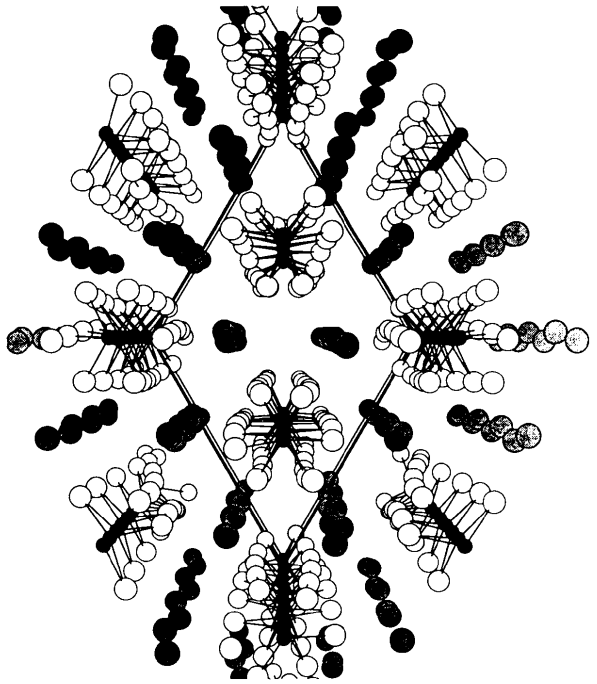

Fig. 3. A perspective view of the modulated structure along the *c* axis. The atom key is same as that in Fig. 2.

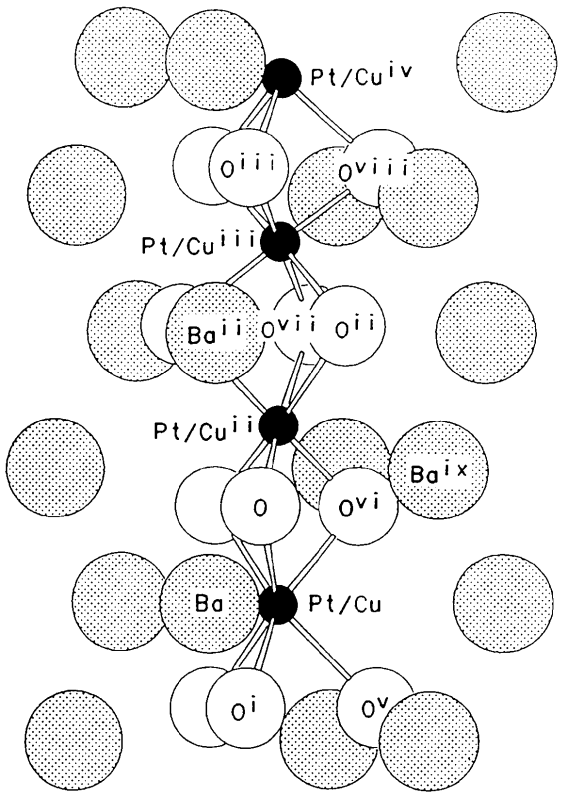

Fig. 4. A part of a $[(Pt,Cu)O_3]_\infty$ column and the surrounding Ba ions. The atom key is same as that in Fig. 2.

Table 3. *Interatomic distances* (Å) *and angles* (°)

Ba—Ba^{ii}	4.22 (1)	Ba—Ba^{ix}	4.22 (2)
Ba^{ii}—Ba^{ix}	4.10 (2)	Ba—Pt/Cu	3.59 (2)
Ba^{ix}—Pt/Cu^{ii}	3.65 (1)	Ba—O	2.73 (8)
Ba^{ii}—O	3.33 (7)	Ba^{ix}—O	3.11 (7)
Pt/Cu—Pt/Cu^{ii}	2.82 (2)	Pt/Cu^{ii}—Pt/Cu^{iii}	2.84 (2)
Pt/Cu^{iii}—Pt/Cu^{iv}	2.57 (2)	Pt/Cu—O	2.04 (7)
Pt/Cu—O^{i}	2.26 (7)	Pt/Cu^{ii}—O	1.83 (7)
Pt/Cu^{ii}—O^{ii}	2.20 (6)	Pt/Cu^{iii}—O^{ii}	2.03 (6)
Pt/Cu^{iii}—O^{iii}	1.97 (8)	Pt/Cu^{iv}—O^{iii}	2.13 (7)
O—O^{vi}	2.3 (2)	O^{ii}—O^{viii}	2.7 (1)

O—Pt/Cu—O^{i}	95. (3)	O—Pt/Cu—O^{v}	136. (3)
O—Pt/Cu—O^{vi}	68. (4)	O^{i}—Pt/Cu—O^{v}	75. (3)
O—Pt/Cu^{ii}—O^{ii}	100. (3)	O—Pt/Cu^{ii}—O^{vi}	78. (4)
O—Pt/Cu^{ii}—O^{vii}	175. (3)	O^{ii}—Pt/Cu^{ii}—O^{vii}	76. (3)
O^{ii}—Pt/Cu^{iii}—O^{iii}	93. (3)	O^{ii}—Pt/Cu^{iii}—O^{vii}	84. (3)
O^{iii}—Pt/Cu^{iii}—O^{viii}	176. (3)	O^{iii}—Pt/Cu^{iii}—O^{viii}	89. (4)
O^{iii}—Pt/Cu^{iv}—O^{viii}	81. (4)	Pt/Cu—O—Pt/Cu^{ii}	93. (3)
Pt/Cu^{ii}—O^{ii}—Pt/Cu^{iii}	84. (2)	Pt/Cu^{iii}—O^{iii}—Pt/Cu^{iv}	78. (3)

Symmetry code: (i) $x, y, z-1$; (ii) $x, y, z+1$; (iii) $x, y, z+2$; (iv) $x, y, z+3$; (v) $-y, x-y, z-1$; (vi) $-y, x-y, z$; (vii) $-y, x-y, z+1$; (viii) $-y, x-y, z+2$; (ix) $x, x-y, z+\frac{1}{2}$.

The mechanism of stabilizing the composite crystal structures is not known. In particular, it is interesting how a structure is stabilized, as in the present case, when trigonal and rhombohedral subsystems interpenetrate each other. In the whole structure, the second subsystem $(Pt,Cu)O_3$ forms a framework structure because $(Pt,Cu)O_3$ polyhedra are considered to be bound tightly along the *c* axis. In the channels among $[(Pt,Cu)O_3]_\infty$ columns, Ba atoms are located at positions forming a hexagonal lattice. If we consider the $(Ba)_\infty$ column along the *c* axis which has a period incommensurate to that of $(Pt,Cu)O_3$ and take into account only the interaction between the two subsystems, then each $(Ba)_\infty$ column will have no preferred position along the *c* axis because of the incommensurability. Therefore, a correlation may exist among the $(Ba)_\infty$ columns forming the hexagonal lattice. Similar considerations can be given to the second subsystem. $[(Pt,Cu)O_3]_\infty$ columns are separated by the $(Ba)_\infty$ columns and have no preferred position along the *c* axis. The rhombohedral lattice is considered to be realized by the interaction between the $[(Pt,Cu)O_3]_\infty$ columns, which prefers the rhombohedral lattice to the hexagonal one. If the interaction between the columns is weak and of the order of k_BT, we can expect a phase transition at high temperatures from the ordered structure to a disordered structure in which the positional correlation among the columns is lost. Such a phase transition is observed in $[AsF_6][Hg]_x[Hg]_x$ (Pouget *et al.*, 1978). Therefore, composite crystals may give a variety of phase transitions, which have not been studied enough.

We thank Y. Saito for the EDX analysis. Our thanks are also due to Professor H. Horiuchi (University of Tokyo) for the use of the EDX analyzer facilities.

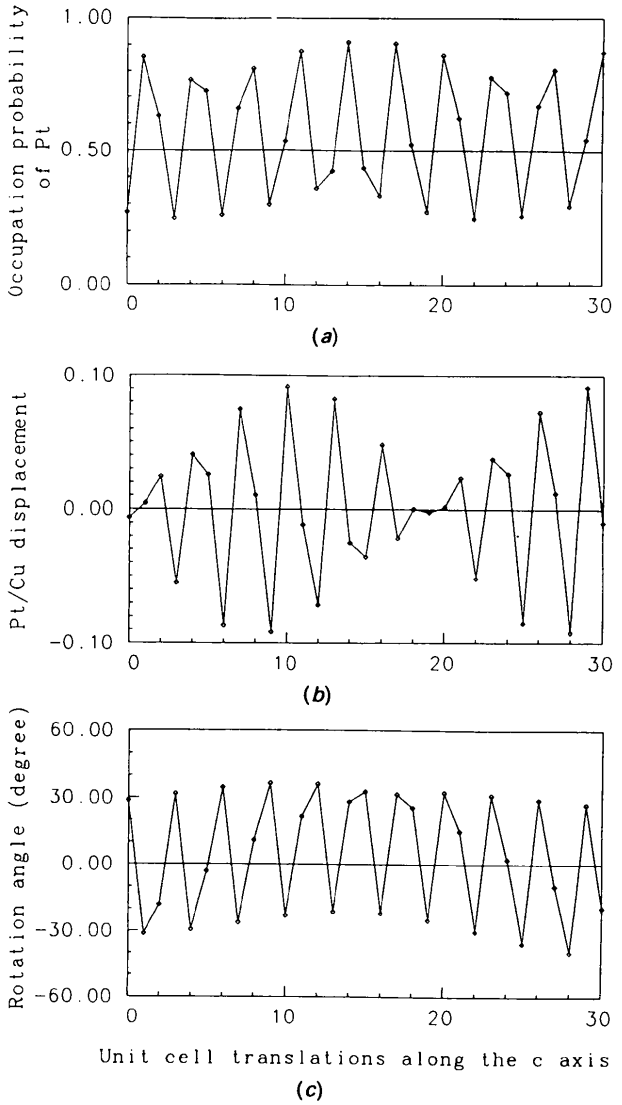

Fig. 5. Plots of the variations of the following quantities *versus* unit-cell translations along the *c* axis: (*a*) occupation probability of Pt atoms, (*b*) displacement of Pt/Cu parallel to the *c* axis, (*c*) rotation angle of O around the *c* axis from the mirror plane. Lines are guides for eyes.

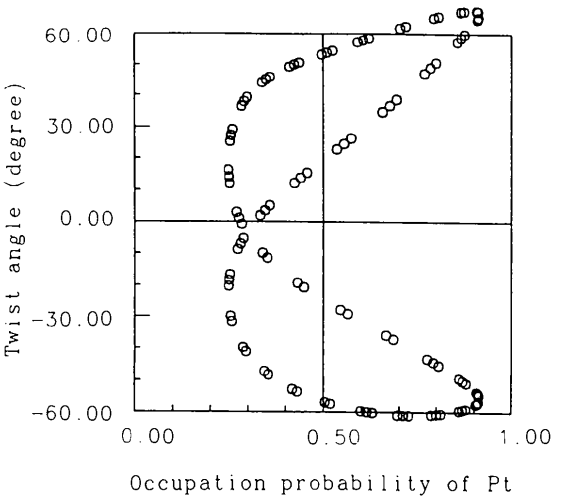

Fig. 6. A plot of the correlation of the twist angle of two triangles of O atoms adjacent to a Pt/Cu atom with the occupation of the Pt/Cu atom.

References

COPPENS, P., GURU ROW, T. N., LEUNG, P., STEVENS, E. D., BECKER, P. J. & YANG, Y. W. (1979). *Acta Cryst.* A**35**, 63–72.

JANNER, A. & JANSSEN, T. (1980). *Acta Cryst.* A**36**, 408–415.

KATO, K. (1990). *Acta Cryst.* B**46**, 39–44.

ONODA, M. & KATO, K. (1991). *Acta Cryst.* B**47**, 630–634.

ONODA, M., KATO, K., GOTOH, Y. & OOSAWA, Y. (1990). *Acta Cryst.* B**46**, 487–492.

POUGET, J. P., SHIRANE, G., HASTINGS, J. M., HEEGER, A. J., MIRO, N. D. & MACDIARMID, A. G. (1978). *Phys. Rev. B*, **18**, 3645–3656.

SAKURAI, T. & KOBAYASHI, K. (1979). *Rikagaku Kenkyusho Hokoku*, **55**, 69–77.

SHISHIDO, T., UKEI, K., SAITO, Y. & FUKUDA, T. (1992). In preparation.

SMAALEN, S. VAN (1989). *J. Phys. Condens. Mater*, **1**, 2789–2800.

TOKONAMI, M. (1965). *Acta Cryst.* **19**, 486.

WOLFF, P. M. DE, JANSSEN, T. & JANNER, A. (1981). *Acta Cryst.* A**37**, 625–636.

YAMAMOTO, A. (1982*a*). *Acta Cryst.* A**38**, 87–92.

YAMAMOTO, A. (1982*b*). *Acta Cryst.* B**38**, 1446–1451, 1451–1456.

YAMAMOTO, A. (1992). *Acta Cryst.* A**48**, 476–483.

YAMAMOTO, A. & NAKAZAWA, H. (1981). *Acta Cryst.* A**37**, 838–842.

YAO, J.-X. (1981). *Acta Cryst.* A**37**, 642–644.